J Mater Sci (2012) 47:315–322
DOI 10.1007/s10853-011-5800-5

Electrosynthesis and characterization of a polyfluorene derivative with green-light-emitting property

Baoyang Lu · Jiong Wang · Ruirui Yue · Jingkun Xu · Meishan Pei

Received: 14 September 2010 / Accepted: 16 July 2011 / Published online: 29 July 2011

Abstract Green-light-emitting poly(diphenylmethylene-fluorene) (PDPMF) was synthesized electrochemically by direct anodic oxidation of diphenylmethylenefluorene (DPMF) in dichloromethane (CH_2Cl_2) and boron trifluoride diethyl etherate (BFEE) binary solution. The oxidation potential of DPMF in this medium was measured to be only 0.78 V versus Ag/AgCl, which was lower than that determined in CH_2Cl_2 (1.0 V versus Ag/AgCl) or acetonitrile (ACN) (1.16 V versus Ag/AgCl) with 0.1 mol L^{-1} tetrabutylammonium tetrafluoroborate (Bu_4NBF_4) as the supporting electrolyte. The as-formed PDPMF films showed good electrochemical behavior and high thermal stability. Fluorescent spectra indicate that PDPMF is a good green-light-emitter with strong and bright green or yellow-green photoluminescence under 365 nm UV light.

Introduction

Since the synthesis of the first polyfluorene in 1985 [1, 2], polyfluorene derivatives (PFs), as one of the few available blue-emitting conjugated polymers, have been demonstrated to be of interest owing to the fact that they present many of the requisite features for light-emitting materials, such as high photoluminescence efficiency, high hole mobility, and good photostability [3–5]. Among the PFs, some mono- and di- substituted polyfluorene appears that disubstituted polymers are of great interest, because of its chemical and thermal stability as well as high fluorescence quantum yields [6, 7], subjected to a variety of applications such as electrochromic materials, cation complexing materials, and also as electrode surface modifiers, especially in light electroluminescent diode (LED) devices [8–10]. On the other side, in recent years PFs with a variety of functional groups in the side chains such as ionic groups or special receptors have been used in several fields such as chemo/biosensors [11–17], polymer light-emitting diodes (PLEDs) [18–20].

PFs were mainly prepared by two main routes, chemical approaches through Suzuki, Yamamoto, and Stille reactions [21] and electrochemical oxidative polymerization of corresponding monomers. In particular, the electro-oxidative polymerization of the heterocycle aromatic compounds with concurrent polymer films deposition has been proved to be an especially useful method for the preparation of conducting polymer films. Previous studies indicated that the quality of PFs films prepared in common organic solvents, such as ionic liquids, acetonitrile (ACN), and CH_2Cl_2, was very poor, usually in the form of powders, insoluble and infusible [22, 23, 33]. It is well-known that free-standing films of PFs can be produced by direct anodic oxidation of corresponding monomers in boron trifluoride diethyl etherate (BFEE) with good mechanical, electrical, and thermal properties. The reason lies in that the interactions between the middle strong Lewis acid (BFEE) and the aromatic monomers can lower their oxidation potentials and the catalytic effect of BFEE facilitates the formation of high quality free-standing polymer films [24–28].

Although anodic oxidation of diphenylmethylenefluorene (DPMF) (Scheme 1) has been reported in CH_2Cl_2–Bu_4NBF_4 (0.2 mol L^{-1}) [29], there was not a systematic

B. Lu · R. Yue · J. Xu (✉)
School of Pharmacy, Jiangxi Science & Technology Normal University, Nanchang 330013, China
e-mail: xujingkun@tsinghua.org.cn

J. Wang · M. Pei (✉)
School of Chemistry and Chemical Engineering, University of Jinan, Jinan 250022, China
e-mail: chm_peims@ujn.edu.cn

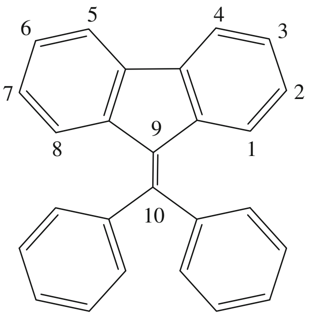

Scheme 1 Chemical structure of DPMF

study of electrodeposited poly(diphenylmethylenefluorene) (PDPMF) film. The main reason probably results from the complicated conditions required for DPMF polymerization, for example, high oxidation potentials needed in common organic media such as acetonitrile, and CH_2Cl_2 generally lead to the poor quality of polymer films.

In this article, the electropolymerization of DPMF in BFEE containing certain amounts of CH_2Cl_2 was carried out. The fluorescence and electrochemical properties, thermal stability, and structure of the as-prepared PDPMF films were also investigated in detail.

Experimental

Reagents and treatment

DPMF (98%; Alsa Aesar) was used as received. BFEE (Beijing Changyang Chemical Plant) was distilled before use. Commercial HPLC grade ACN (Tianjin Guangfu Fine Chemical Research Institute, China) was used directly without further purification. CH_2Cl_2 and 25% ammonia were made by Beijing Chemical Plant. Bu_4NBF_4 (95%; Acros Organics) was dried under vacuum at 60 °C for 24 h before use. Other reagents were all analytical grade and used as received.

Apparatus

UV–vis spectra were taken by using a Perkin-Elmer Lamda 900 UV–vis–NIR spectrophotometer. IR spectra were recorded by using KBr pellets of the polymers on a Bruker Vertex 70 FT–IR spectrometer. Thermogravimetric analysis (TGA) was performed with a Pyris Diamond TG/DTA thermal analyzer (PerkinElmer). With an F-4500 fluorescence spectrophotometer (Hitachi), the fluorescence spectra were determined. The fluorescence quantum yield (ϕ_{overall}) in solution was measured using anthracene in ACN (standard, $\phi_{\text{ref}} = 0.27$) as a reference and was calculated according to the well-known method given as Eq. 1 [30].

$$\phi_{\text{overall}} = \frac{n^2 A_{\text{ref}} I}{n_{ref}^2 A I_{\text{ref}}} \times \phi_{\text{ref}} \tag{1}$$

Here, n, A, and I denote the refractive index of solvent, the absorbance at the excitation wavelength, and the intensity of the emission spectrum, respectively. The subscript “ref” denotes the reference, and no subscript denotes the sample. Absorbance of the samples and the standard should be similar.

Electrosynthesis of the polymer films

The electrochemical polymerization and examinations were performed in a one-compartment cell by the use of a Model 263 potentiostat–galvanostat (EG&G Princeton Applied Research) under computer control at room temperature. The cyclic voltammetric experiments were investigated using a platinum electrode as the working electrode with a diameter of 0.05 cm, which was carefully polished with abrasive paper (1500 mesh) and cleaned by water and acetone successively before each examination. The counter electrode was a stainless steel wire. To obtain a sufficient amount of polymer for characterization, platinum sheet, and stainless steel sheet with surface area of 4 and 6 cm^2 each were employed as the working and counter electrodes, respectively. All potentials were referred to an Ag/AgCl electrode immersed directly in the solution. The typical electrolytic solution was CH_2Cl_2 containing BFEE (It should be noted that BFEE was used as the supporting electrolyte in CH_2Cl_2 solutions without any other salts). All solutions were deaerated by a dry argon stream and maintained at a slight argon overpressure during the experiments. After polymerization, the polymers were scraped from the electrode surface and then washed repeatedly with acetone to remove the electrolyte and monomer. For spectral studies, PDPMF films were dedoped with 25% ammonia for 3 days and then washed repeatedly with distilled water and acetone. Finally, they were dried under vacuum at 60 °C for 2 days.

Results and discussion

Electrochemical polymerization of DPMF

The anodic polarization curves of DPMF in CH_2Cl_2–BFEE (5:3, v/v; A), ACN–Bu_4NBF_4 (B), and CH_2Cl_2–Bu_4NBF_4 (inset) are shown in Fig. 1. The concentration of Bu_4NBF_4 in both ACN and CH_2Cl_2 is 0.1 mol L^{-1}. The oxidation of DPMF all exhibited three anodic waves in CH_2Cl_2–BFEE (A), ACN–Bu_4NBF_4 (B), and CH_2Cl_2–Bu_4NBF_4 (inset). It is clear from the curve that a rapid growth of the anodic current density started around 0.78 V

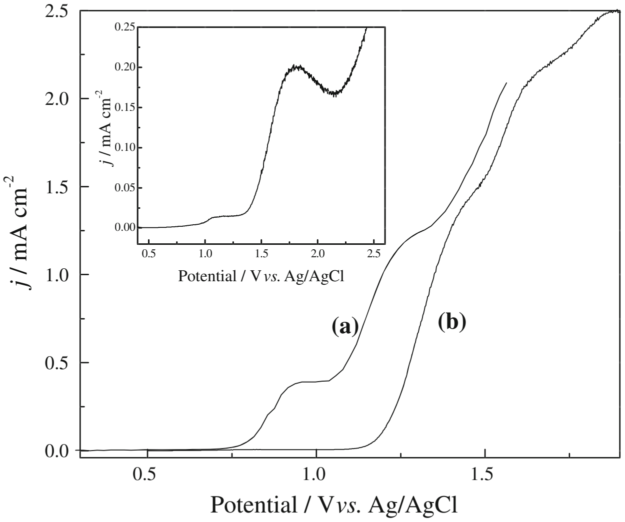

Fig. 1 Anodic polarization curves of DPMF in CH_2Cl_2–BFEE (*a*) (5:3, v/v), ACN–Bu_4NBF_4 (*b*), and CH_2Cl_2–Bu_4NBF_4 (*inset*), respectively. Potential scan rate: 100 mV s^{-1}

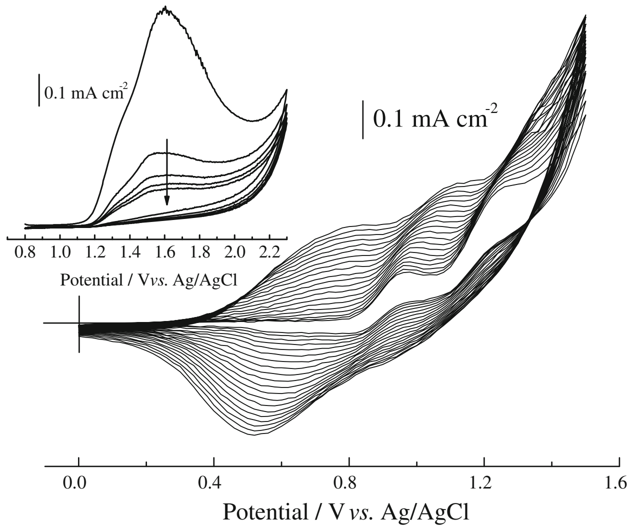

Fig. 2 Cyclic voltammograms of 0.01 mol L^{-1} DPMF in CH_2Cl_2–BFEE (5:3, v/v) and ACN–Bu_4NBF_4 (*inset*). Potential scan rate: 100 mV s^{-1}

and the next at about 1.06 V in CH_2Cl_2–BFEE binary solution (Fig. 1a), which are much lower than those observed in ACN–Bu_4NBF_4 (1.16 and 1.50 V) (Fig. 1b) or CH_2Cl_2–Bu_4NBF_4 (1.0 and 1.34 V) (Fig. 1 inset). This distinct decrease of the oxidation potentials in CH_2Cl_2–BFEE can be attributable to the specific catalytic effect of BFEE, which facilitates the anodic oxidation of DPMF.

Cyclic voltammetry (CV) is a very useful method which qualitatively reveals the reversibility of electron transfer during the electropolymerization and also examines the electroactivity of the polymer film because the oxidation and reduction can be monitored in the form of a current–potential diagram [31]. Figure 2 displays cyclic voltammograms (CVs) of DPMF on a platinum electrode in CH_2Cl_2–BFEE and ACN–Bu_4NBF_4 (inset) by potential scanning. In CH_2Cl_2–BFEE, PDPMF films can be reduced and oxidized between 0.50 and 1.20 V. Upon sequential cycles, redox currents increased, implying the formation of an electro active and conductive layer on the platinum electrode surface (yellow to black as the deposit thickened). At the same time, a coloration of the solution occurred due to the concomitant formation of soluble oligomers. Moreover, the oxidation onset potential progressively decreased as the scanning cycles increased, reflecting that more and more monomers coupled on the electrode surface and led to an increase of the number of monomeric units in the polymer chain [32].

Compared to CVs recorded in CH_2Cl_2–BFEE, CVs of DPMF in ACN–Bu_4NBF_4 (Fig. 2 inset) were quite different. A strong irreversible oxidation can be found in the potential range from 1.10 to 2.10 V on the first cycle. However, the anodic current intensity decreased quickly on the following cycles. No polymer was observed on the electrode surface and the solution remained transparent during the electrolysis process. This is in accordance with the results reported previously by Rault-Berthelot et al. [29]. In this regard, ACN–Bu_4NBF_4 is not a good medium for the electropolymerization of DPMF because the high oxidation potential needed leads to overoxidation and more defects on the polymer films. Therefore, CH_2Cl_2–BFEE is a better choice and the polymer films used for the following characterization were all prepared potentiostatically in this medium at a constant applied potential of 1.40 V versus Ag/AgCl.

Electrochemistry of PDPMF films

Figure 3 shows the CVs of PDPMF films obtained from CH_2Cl_2–BFEE binary solution in different monomer-free media. Similar to the results in the literature [33], the steady-state CVs represented broad anodic and cathodic peaks. In monomer-free BFEE (Fig. 3a), the oxidation and reduction of PDPMF films occurred at 0.76 and 0.56 V at the potential scan rate of 25 mV s^{-1}, respectively. With the scan rates increasing, the potentials needed to oxidize and reduce the polymer film shifted positively and negatively to about 1.00 and 0.42 V, respectively. This can be mainly ascribed to the slow transfer rate of large doping anions and solvent molecules in BFEE, such as $(EtO)_3BF_3^-$, especially at higher scan rates [29]. Furthermore, the film was cycled repeatedly without significant loss of electroactivity. In concentrated sulfuric acid, the redox potentials of the polymer films were very stable versus potential scan rates (Fig. 3b). It could be oxidized and reduced from 0.75 to

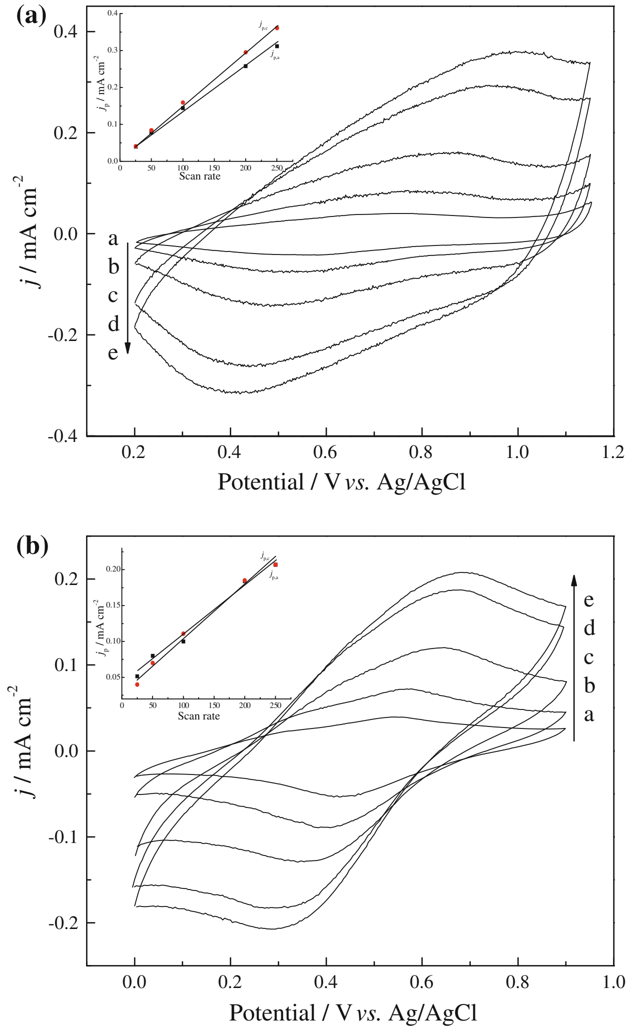

Fig. 3 Cyclic voltammograms of PDPMF films in BFEE (**a**) and concentrated sulfuric acid (**b**) at potential scan rates of 25 mV s^{-1} (*a*), 50 mV s^{-1} (*b*), 100 mV s^{-1} (*c*), 150 mV s^{-1} (*d*), 200 mV s^{-1} (*e*). PDPMF films were both synthesized potentiostatically at 1.40 V versus Ag/AgCl in CH_2Cl_2−BFEE (5:3, v/v). *Inset* plots of redox peak current densities versus potential scan rates. j_p is the peak current densities, and $j_{p,a}$ and $j_{p,c}$ denote the anodic and cathodic peak current densities, respectively

0.25 V and could be cycled repeatedly between the conducting (oxidized) and insulating (neutral) state without significant decomposition of the materials. From the above results, PDPMF films from CH_2Cl_2−BFEE showed good redox activity and stability.

Structural characterization

Infrared spectra can provide much structural information for polymers, especially for insoluble, and infusible polymers. A comparison of the evolution of the vibrational modes appearing in polymers and in some simpler related molecules acting as references usually facilitates the interpretation of the experimental absorption spectra. Figure 4 shows the transmittance FT–IR spectra of the DPMF monomer (Fig. 4a) and dedoped PDPMF films (Fig. 4b). Compared with fluorene [34], some small bands are unique for DPMF. For example, the C=C stretching vibration of DPMF extends to 1680–1660 cm^{-1} (Fig. 4a). Most of these vibration bands can be seen after polymerization in the IR spectrum of the polymer (Fig. 4b). The conservation of most of the bands proves the structure of the monomer to be conserved after polymerization. From Fig. 4b, the characteristic band at 1690–1636 cm^{-1} was the typical absorption of C=C stretching. The 1400 and 692 cm^{-1} peaks were ascribed to the C–H wagging vibration on aromatic rings. PDPMF also displayed three bands centered at 818, 760, and 700 cm^{-1}, indicating the existence of 1,2,4-trisubstituted phenyl ring [35]. This implies the polymerization of DPMF occurs at 2,7 or 3,6 positions.

Now quantum chemistry calculation has been used to investigate the chemical structure and properties in many fields, for example, polymer science, materials science [32, 39, 43, 44], and environmental science [36–38]. In order to gain further insight into the structure of PDPMF and the polymerization mechanism, main atomic electron density population and proportion of the frontier orbitals of the DPMF monomer (Table 1, Scheme 2) and electron spin density of $DPMF^{\cdot +}$ (Table 2) were calculated at the B3LYP/6-31G(d, p) level using Gaussian 03 software. The results of main atomic electron density population reveal negative electric charges mainly on $C_{(1)}$, $C_{(2)}$, $C_{(3)}$, $C_{(4)}$, $C_{(5)}$, $C_{(6)}$, $C_{(7)}$, and $C_{(8)}$ (Table 1), which implied that these atoms may donate electrons during electrochemical polymerization through radical cation intermediates. According to the molecular orbital theory, the reaction

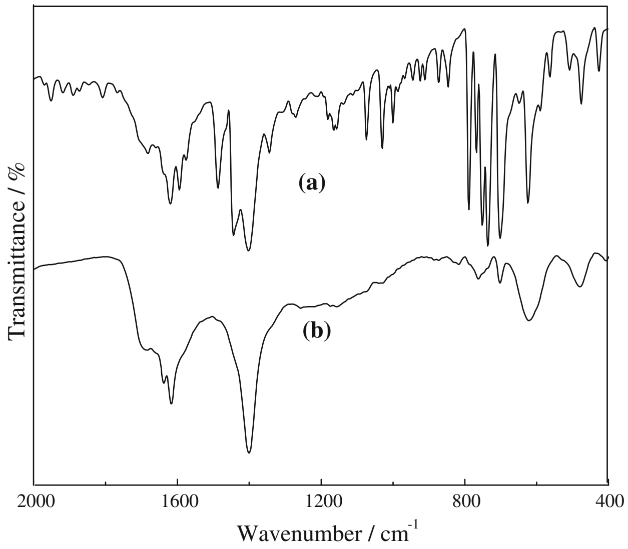

Fig. 4 FT–IR spectra of DPMF (*a*) and dedoped PDPMF (*b*)

Table 1 Main atomic electron density populations for DPMF

Atom	Electric charge	Atom	Electric charge
$C_{(1)}$	−0.131116	$C_{(2)}$	−0.095534
$C_{(3)}$	−0.093860	$C_{(4)}$	−0.125466
$C_{(5)}$	−0.125719	$C_{(6)}$	−0.093654
$C_{(7)}$	−0.095533	$C_{(8)}$	−0.131565
$C_{(9)}$	0.035049	$C_{(10)}$	−0.079568

Table 2 Main atomic electron spin densities for DPMF$^{\cdot+}$

Atom	Electron spin density	Atom	Electron spin density
$C_{(1)}$	0.124562	$C_{(2)}$	−0.057004
$C_{(3)}$	0.121669	$C_{(4)}$	0.000973
$C_{(5)}$	0.001048	$C_{(6)}$	0.121564
$C_{(7)}$	−0.056953	$C_{(8)}$	0.124549
$C_{(9)}$	0.254335	$C_{(10)}$	0.181201

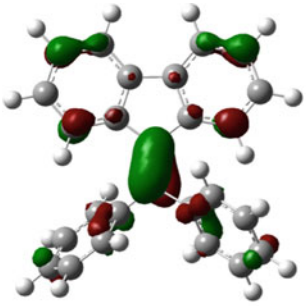

HOMO

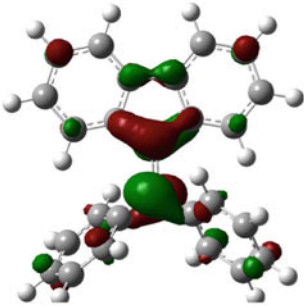

LUMO

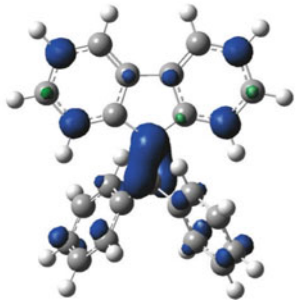

ESD

Scheme 2 Main composition of HOMO and LUMO in DPMF monomer and atomic electron spin densities (ESD) for DPMF$^{\cdot+}$ (without H atoms)

between the active molecules mainly happens on the frontier molecular orbital and the near orbital. For DPMF, the proportions of atoms $C_{(1)}$, $C_{(3)}$, $C_{(6)}$, $C_{(8)}$, and $C_{(9)}$ in the HOMO were higher than other atoms (Scheme 2). However, there will be significant steric hindrance effect when coupling at $C_{(1)}$, $C_{(8)}$, and $C_{(9)}$ positions. On the other hand, electron spin density of the monomer radical cation is the main factor controlling the electropolymerization according to many authors [40–42]. The relatively higher atomic electron density of DPMF$^{\cdot+}$ can be seen at $C_{(1)}$, $C_{(3)}$, $C_{(6)}$, $C_{(8)}$, $C_{(9)}$, and $C_{(10)}$ positions (Table 2), indicating higher propensity for radical-coupling and bond formation at these positions. Based on all these calculated results, it can be reasonably deduced that the polymerization between the monomer would happen preferentially on $C_{(3)}$ and $C_{(6)}$, well in accordance with FT–IR results mentioned previously. This is quite different from the results for many polyfluorenes by electropolymerization reported previously (the electropolymerization happens mainly at $C_{(2)}$ and $C_{(7)}$ of fluorenes) [22–28, 33].

UV–vis and fluorescence spectra

Both doped and dedoped PDPMF films are partly soluble in polar organic solvents such as DMSO. The UV–vis spectra of DPMF and PDPMF dissolved in DMSO were examined, as shown in Fig. 5. The monomer showed a characteristic absorption peak at 320 nm (Fig. 5a), which was assigned to a single-electron π–π^* transition of aromatic rings. However, the spectra of the doped and dedoped PDPMF films showed a much broader absorption at 353 (Fig. 5b) and 352 nm (Fig. 5c), respectively. The overall absorption of PDPMF tailed off to more than 600 nm (Fig. 5b, c). In general, the longer wavelength is the absorption, the higher conjugation length is the polymer [43–45]. These spectral results confirmed the occurrence of electrochemical polymerization among the monomers and the formation of a conjugated polymer with broad molar mass distribution.

Fluorescence spectra of the doped and dedoped polymers were both determined in DMSO (the soluble part) and in the solid state on ITO electrode, as shown in Fig. 6. DPMF exhibited a strong peak at about 338 nm (Fig. 6a). In comparison, the emission peaks of the doped (Fig. 6b) and dedoped (Fig. 6c) PDPMF located at 511 and 507 nm, much longer than other blue light-emitting polyfluorenes, such as poly(9-hydroxyfluorene) with 381 nm, poly(9-fluorenecarboxylic acid) with 430 nm, poly(9-hydroxy-9-fluorenecarboxylic acid) with 408 nm, and poly(9-aminofluorene) with 408 nm [47, 48]. The wider emission spectra of the polymer compared with that of the monomer can be

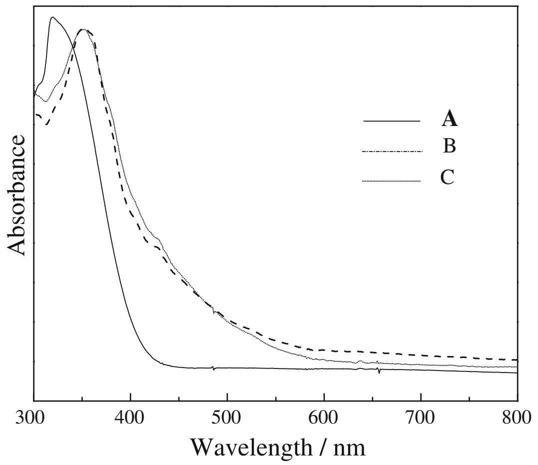

Fig. 5 UV–vis spectra of DPMF (*A*), doped PDPMF (*B*), and dedoped PDPMF (*C*) in DMSO

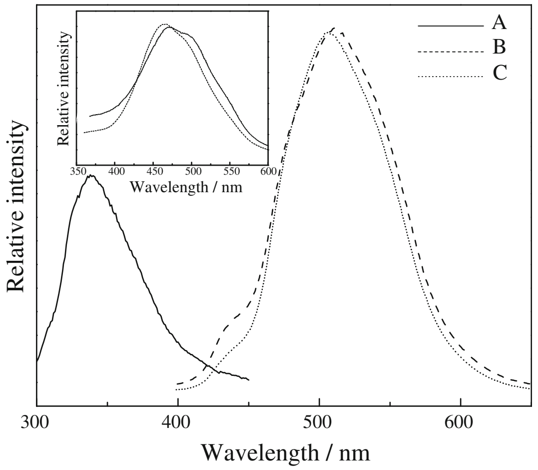

Fig. 6 Emission spectra of DPMF (*A*), doped PDPMF (*B*), and dedoped PDPMF (*C*) in DMSO. *Inset* Emission spectra of PDPMF prepared at a constant applied potential of 1.40 V versus Ag/AgCl for 200 s on the ITO transparent electrode

ascribed to the wide molar mass distribution of PDPMF, in accordance with UV–vis spectra. Doped and dedoped (Fig. 6 inset) PDPMF deposited on ITO transparent electrode showed an emission peak at about 470 nm, quite different from those in solution. The blue shift of the emission spectra of PDPMF film in solid state may be attributed to the interaction of adjacent polymer chains in polymer matrix. Meanwhile, it is also very interesting to find that soluble PDPMF dissolved in common organic solvents can all emit a strong and bright green photoluminescence when exposed to 365 nm UV light (Fig. 7b, c), whereas the monomer showed no emission (Fig. 7a). According to Eq. 1, the fluorescence quantum yield (ϕ_{overall}) of DPMF monomer was calculated to be only 0.01, whereas those of the doped and dedoped PDPMF films prepared from CH_2Cl_2–BFEE were significantly improved to 0.09 and 0.11, respectively. These values are relatively low in comparison with other polyfluorenes, such as poly(9-aminofluorene) (0.40) [48]. However, as a green-light-emitter, PDPMF may find other applications in various fields compared with other blue light-emitting polyfluorenes.

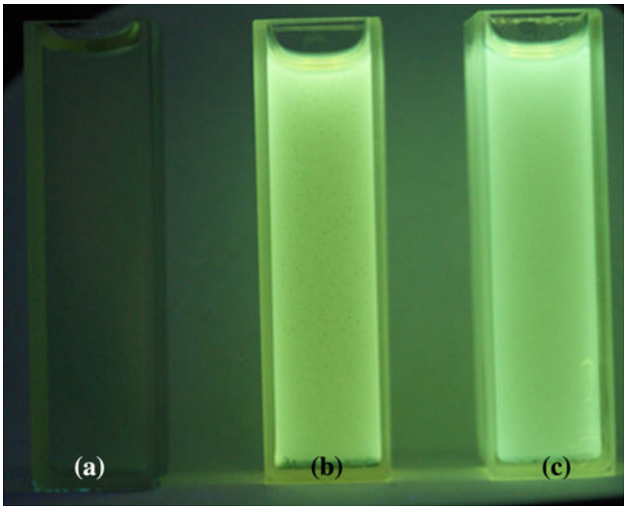

Fig. 7 Photograph of DPMF (*a*), doped PDPMF (*b*), and dedoped PDPMF (*c*) in DMSO under 365 nm UV irradiation

Thermal analysis

The thermal stability of a polymer is very important for its potential applications. Thermogravimetric (TG) analysis is a significant and useful dynamic way to detect the degradation behavior in which the weight loss of a polymer sample is measured continuously while the temperature is changed at a constant rate. It is known that the skeletal decomposition temperature of polymers is usually low, which hinders the practical use of these polymers in various fields. To investigate the thermal stability of PDPMF films, thermogravimetric experiments were performed under a nitrogen stream at a heating rate of 10 K min^{-1}. Figure 8 shows the TG (A) and DTG (B) curves of dedoped PDPMF films obtained from the binary solvent system. At low temperatures ($T < 440$ K), the polymer initially underwent a small weight decrease of about 0.23%, which may be attributed to water evaporation or other moisture trapped in the polymer according to many authors [46]. From 440 to 590 K, the polymer proceeded to a rapid weight loss of 39.34%. Simultaneously, from the DTG curve (Fig. 8b), the corresponding maximal decomposition existed at 565 K. Such a prominent weight loss was closely related to the oxidizing decomposition of the PDPMF chain structure. The following degradation after

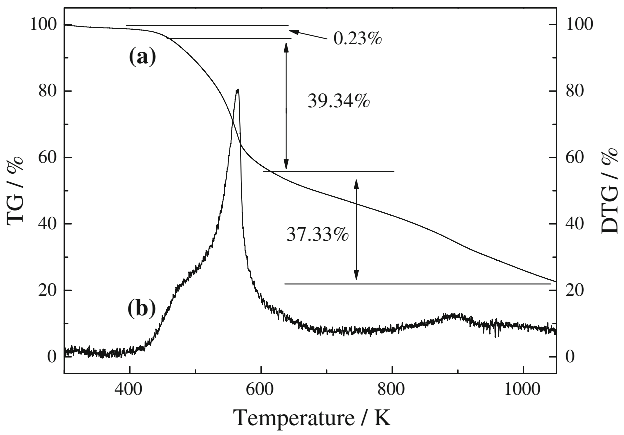

Fig. 8 TG (*A*) and DTG (*B*) curves of dedoped PDPMF films

590 K was probably caused by the overflow of the oligomers decomposed from PDPMF. In comparison with other polyfluorenes we reported previously, the thermal stability of PDPMF is better than that of poly(9-hydroxyfluorene), poly(9-fluorenecarboxylic acid), poly(9-hydroxy-9-fluorenecarboxylic acid) [47], and poly(9-aminofluorene) [48], but worse than polyfluorene [34]. The relatively high decomposition temperature of the polymer films suggests a wider temperature scale for their potential applications.

Conclusions

Green-light-emitting PDPMF with redox activity and stability was successfully electrosynthesized in CH_2Cl_2–BFEE binary solvent system. As-prepared PDPMF films are green-light-emitting materials and emit a strong and bright green photoluminescence under 365 nm UV light. UV–vis and FT–IR spectral results, together with quantum chemistry calculations, demonstrated that the electrochemical polymerization of DPMF probably occurs via the coupling at $C_{(3)}$ and $C_{(6)}$ positions. Also favorable thermal stability makes PDPMF probably a promising candidate as a green-light-emitter used in many specific fields, such as luminophore in liquid crystalline systems.

Acknowledgements NSFC (50963002, 51073074), Jiangxi Provincial Department of Education (GJJ11590, GJJ10678), Natural Science Foundation of Jiangxi Province (2010GZH0041), Jiangxi Science & Technology Normal University (KY2010ZY13), and Key Laboratory of Photochemical Conversion and Optoelectronic Materials, TIPC, CAS are acknowledged for their financial support.

References

1. Rault-Berthelot J, Simonet J (1995) J Electroanal Chem 182:187
2. Rault-Berthelot J, Simonet J (1986) New J Chem 10:169
3. Wu FL, Shih PL, Shu CF, Tung YL, Chi Y (2005) Macromolecules 38:9028
4. Yang Y, Pei QB (1997) J Appl Phys 81:3294
5. Liu B, Yu WL, Lai YH, Huang W (2001) Chem Mater 13:1984
6. Klaerner G, Lee JI, Davey MH, Miller RD (1999) Adv Mater 11:115
7. Byun HY, Chung IJ, Shim HK, Kim CY (2004) Chem Phys Lett 393:197
8. Leclerc M (2001) J Polym Sci Part A Polym Chem 39:2867
9. Rault-Berthelot J, Angely L, Delaunay J, Simonet J (1987) New J Chem 11:487
10. Rault-Berthelot J, Questaigne V, Simonet J (1989) New J Chem 13:45
11. Liu B, Bazan GC (2006) J Am Chem Soc 128:1188
12. Wang S, Gaylord BS, Bazan GC (2004) J Am Chem Soc 126:5446
13. Liu B, Wang S, Bazan GC, Mikhailovsky A (2003) J Am Chem Soc 125:13306
14. Fan CH, Plaxco KW, Heeger AJ (2002) J Am Chem Soc 124:5642
15. Zhou G, Cheng YX, Wang LX, Jing XB, Wang FS (2005) Macromolecules 38:2148
16. Zhou XH, Yan JC, Pei J (2004) Macromolecules 37:7078
17. Zhou G, Qian G, Ma L, Cheng YX, Xie ZY, Wang LX, Jing XB, Wang FS (2005) Macromolecules 38:5416
18. Huang F, Hou LT, Wu HB, Wang XH, Shen HL, Cao W, Yang W, Cao Y (2004) J Am Chem Soc 126:9845
19. Wu H, Huang F, Mo Y, Yang W, Wang D, Peng J, Cao Y (2004) Adv Mater 16:1826
20. Yang RQ, Wu HB, Cao Y, Bazan GC (2006) J Am Chem Soc 128:14422
21. Scherf U, List EJW (2002) Adv Mater 14:477
22. Zhang SS, Nie GM, Han XJ, Xu JK, Li MS, Cai T (2006) Electrochim Acta 51:5738
23. Xu JK, Zhang YJ, Wei ZH, Zhou WQ, Zhao JQ (2006) Acta Chim Sin 64:911
24. Fang Q, Yamamoto T (2004) Macromolecules 37:5894
25. Wang XC, Yue RR, Lu BY, Wei ZH, Xu JK (2010) J Mater Sci 45:1963. doi:10.1007/s10853-009-4188-y
26. Liu XM, He CB, Hao XT, Tan LW, Li YQ, Ong KS (2004) Macromolecules 37:5965
27. Banach MJ, Friend RH, Sirringhaus H (2004) Macromolecules 37:6079
28. Wei ZH, Xu JK, Zeng LQ, Le ZG, Shen L, Pu SZ (2008) J Mater Sci 43:1008. doi:10.1007/s10853-007-2234-1
29. Rault-Berthelot J, Granger MM (1993) J Electroanal Chem 353:341
30. Lakowicz JR (1999) Principles of fluorescence spectroscopy, 2nd edn. Kluwer Academic/Plenum, New York
31. Li XG, Huang MR, Duan W, Yang YL (2002) Chem Rev 102:2925
32. Dong B, Song DF, Zheng LQ, Xu JK, Li N (2009) J Electroanal Chem 633:63
33. Pandey PC, Prakash R (1998) J Electrochem Soc 145:4103
34. Xu JK, Zhang YJ, Hou J, Wei ZH, Pu SZ, Zhao JQ, Du YK (2006) Eur Polym J 42:1154
35. Zhou M, Heinze J (1999) Electrochim Acta 44:1733
36. Zhang QZ, Yu WN, Zhang RX, Zhou Q, Gao R, Wang WX (2010) Environ Sci Technol 44:3395
37. Xu F, Wang H, Zhang QZ, Zhang RX, Qu XH, Wang WX (2010) Environ Sci Technol 44:1399
38. Zhang QZ, Li SQ, Qu XH, Shi XY, Wang WX (2008) Environ Sci Technol 42:7301
39. Lu BY, Yan J, Xu JK, Zhou SY, Hu XJ (2010) Macromolecules 43:4599
40. Smith JR, Cox PA, Campbell SA, Ratcliffe NM (1995) J Chem Soc Faraday Trans 91:2331
41. Ando S, Ueda M (2002) Synth Met 129:207

42. Doskocz J, Doskocz M, Roszak S, Soloducho J, Leszczynski J (2006) J Phys Chem A 110:13989
43. Lu BY, Xu JK, Fan CL, Miao HM, Shen L (2009) J Phys Chem B 113:37
44. Zeng LQ, Le ZG, Xu JK, Liu HT, Zhao F, Pu SZ (2008) J Mater Sci 43:1135. doi:10.1007/s10853-007-1976-0
45. Yue RR, Xu JK, Lu BY, Liu CC, Li YZ, Zhu ZJ, Chen S (2009) J Mater Sci 44:5909. doi:10.1007/s10853-009-3836-6
46. Thieblemont JC, Brun A, Marty J, Planche MF, Calo P (1995) Polymer 36:1605
47. Fan CL, Xu JK, Chen W, Lu BY, Miao HM, Liu CC, Liu GD (2009) J Phys Chem C 113:9900
48. Fan CL, Xu JK, Chen W, Dong B (2008) J Phys Chem C 112:12012